

Profiling of inhibitory immune checkpoints in glioblastoma: Potential pathogenetic players

SALVO DANILO LOMBARDO¹, ALESSIA BRAMANTI², ROSELLA CIURLEO²,
MARIA SOFIA BASILE², MANUELA PENNISI³, RITA BELLA⁴, KATIA MANGANO³,
PLACIDO BRAMANTI², FERDINANDO NICOLETTI³ and PAOLO FAGONE³

¹CeMM Research Center for Molecular Medicine of the Austrian Academy of Sciences, A-1090 Vienna, Austria;

²IRCCS Centro Neurolesi Bonino Pulejo, I-98124 Messina; Departments of ³Biomedical and Biotechnological Sciences and ⁴Medical Sciences, Surgery and Advanced Technologies, University of Catania, I-95123 Catania, Italy

Received July 30, 2020; Accepted October 6, 2020

DOI: 10.3892/ol.2020.12195

Abstract. Glioblastoma (GBM) represents the most frequent glial tumor, with almost 3 new cases per 100,000 people per year. Despite treatment, the prognosis for GBM patients remains extremely poor, with a median survival of 14.6 months, and a 5-year survival less than 5%. It is generally believed that GBM creates a highly immunosuppressive microenvironment, sustained by the expression of immune-regulatory factors, including inhibitory immune checkpoints, on both infiltrating cells and tumor cells. However, the trials assessing the efficacy of current immune checkpoint inhibitors in GBM are still disappointing. In the present study, the expression levels of several inhibitory immune checkpoints in GBM (CD276, VTCN1, CD47, PVR, TNFRSF14, CD200, LGALS9, NECTIN2 and CD48) were characterized in order to evaluate their potential as prognostic and eventually, therapeutic targets. Among the investigated immune checkpoints, TNFRSF14 and NECTIN2 were identified as the most promising targets in GBM. In particular, a higher TNFRSF14 expression was associated with worse overall survival and disease-free survival, and with a lower Th1 response.

Introduction

According to the World Health Organization (WHO) classification of the central nervous system (CNS) tumors, glioblastoma (GBM) is defined as a grade IV astrocytoma (1). GBM represents the most malignant glioma and it is characterized by necrosis, neovascularization and histological heterogeneity (2). GBM represents the most frequent glial tumor, with almost 3 new cases per 100,000 people per year (3). The current stan-

dard of care for GBM consists of surgical resection, followed by radiotherapy and chemotherapy with temozolomide (4). Despite treatment, the prognosis for GBM patients remains extremely poor, with a median survival period of 14.6 months, and the 5-year survival is less than 5% (4).

In recent years, great progress has been made in the area of immunotherapy and accumulating preclinical and clinical data seem to suggest potential novel therapeutic avenues for GBM patients (5,6). It is generally believed that GBM creates a highly immunosuppressive/immunoregulatory microenvironment. Several checkpoint molecules capable of inhibiting the immune responses against neo-antigens, including CTLA4 and PD1/PDL-1, are expressed on both T cells and cancer cells. Immune checkpoint inhibitors, such as nivolumab, ipilimumab and pembrolizumab, have strikingly improved patient survival in solid tumors, such as non-small lung cancer and melanoma. However, the trials assessing the efficacy of immune checkpoint inhibitors in GBM are still disappointing (7). A retrospective study of the use of pembrolizumab in the treatment of recurrent CNS tumors, including GBM, demonstrated that patients treated with Pembrolizumab did not have improved survival (7). Another Phase III randomized trial comparing radiation and concomitant temozolomide with or without nivolumab showed that no progression-free survival benefits were obtained by the addition of nivolumab. However, in a Phase II trial, preoperative administration of nivolumab increased chemokine expression and T-cell receptor clonal diversity, which likely promotes immune-cell infiltration and antitumor immune response (7).

It is reasonable that targeting multiple immune checkpoints in combination with cytotoxic drugs could represent a promising strategy for GBM. The present study characterized the expression levels of several inhibitory immune checkpoints in GBM (i.e., CD276, VTCN1, CD47, PVR, TNFRSF14, CD200, LGALS9, NECTIN2 and CD48) in order to evaluate their prognostic value. Moreover, their potential effects in regulating immune-cell infiltration was investigated.

Materials and methods

Profiling of inhibitory immune checkpoints in GBM. In order to evaluate the expression levels of inhibitory immune check-

Correspondence to: Dr Paolo Fagone, Department of Biomedical and Biotechnological Sciences, University of Catania, I-95123 Catania, Italy
E-mail: paolofagone@yahoo.it

Key words: glioblastoma, immune checkpoint, inhibitory checkpoints, astrocytoma, CD276, VTCN1, CD47, PVR, TNFRSF14, CD200, LGALS9, NECTIN2, CD48

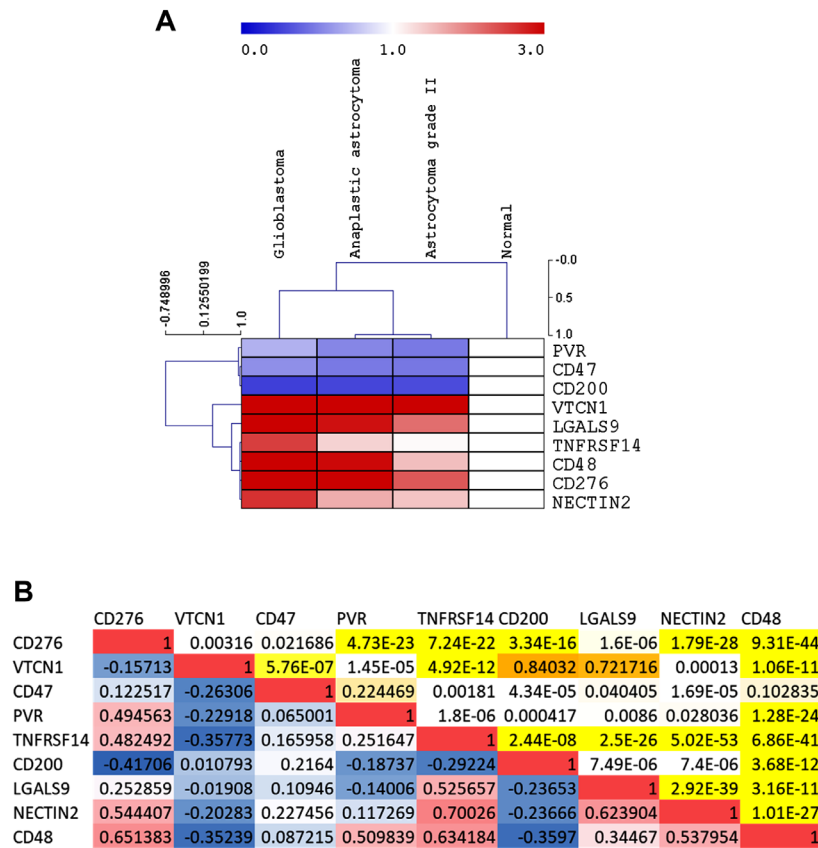


Figure 1. Expression of immune checkpoints in glioblastoma. Relative expression levels of the selected inhibitory immune checkpoints in glioblastoma, lower grade astrocytomas and normal brain samples are presented as heatmap (A). Correlation of the selected inhibitory immune checkpoints (B). Pearson correlation coefficient is presented in blue-red gradient and significance in yellow gradient.

points in GBM as compared to lower grade astrocytomas and normal brain samples, RSEM-normalized RNA Seq data were downloaded from the The Cancer Genome Atlas (TCGA) databank. Selected genes were CD276, VTCN1, CD47, PVR, TNFRSF14, CD200, LGALS9, NECTIN2 and CD48. Complete clinical data of the patients were retrieved and only data from primary tumors, with no neoadjuvant therapy prior to excision, were selected. Data were subjected to logarithmic transformation and Linear Model for Microarray Analysis (LIMMA) was used to assess statistical significance for the differences among cancer types. Overall, this study comprised 153 GBM samples, 130 anaplastic astrocytoma (grade III) samples, 63 astrocytoma (grade II) samples and 5 normal brain samples. The results shown here are based upon data generated by the TCGA Research Network (<https://www.cancer.gov/tcga>). TCGA Ethics & Policies were originally published by the National Cancer Institute.

Survival analysis. Samples were stratified in quartiles based on the expression of the genes of interest and samples in the upper and lower quartiles were selected for comparison. Kaplan-Meier curves were constructed for overall survival and disease-free survival and its significance analyzed by log-rank (Mantel-Cox) test.

Computational deconvolution of infiltrating immune cells. In order to evaluate the relative proportions of the infiltrating immune cell subsets in GBM samples diverging for the

expression of the selected immune checkpoints and stratified in accordance to survival analysis, we performed a computational deconvolution analysis. The web-based utility, xCell, was used. It is a computational tool that is able, by using gene signatures, to infer the presence in a sample of various cell types, including immature dendritic cells (iDCs), conventional DCs (cDCs), active DCs (aDCs), plasmacytoid DCs (pDCs), B cells, CD4⁺ naive T cells, memory B cells, plasma cells, Th1 cells, Th2 and Treg cells and macrophages (8).

Statistical analysis. Gene expression differences were evaluated using LIMMA on log-transformed RSEM-normalized expression values. FDR <0.05 was considered for statistical significance. Gene expression was visualized as heatmap, using the group mean value. Clustering was performed for both sample groups and genes of interest, using Pearson correlation as distance metrics. Correlation analysis was performed using the Pearson's correlation test. Survival analysis was performed using Kaplan-Meier and its significance analyzed by the log-rank (Mantel-Cox) test. For the analysis, P<0.05 was considered to indicate a statistically significant difference. Statistical analysis was performed with GraphPad Prism 8 (GraphPad Software, Inc.) and SPSS 24 (IBM Corp.).

Results

Expression of inhibitory immune checkpoints in GBM. A significant upregulation in the expression levels of CD276,

Table I. Expression of selected immune checkpoints in gliomas.

	CD276	VTCN1	CD47	PVR	TNFRSF14	CD200	LGALS9	CD48	NECTIN2
Glioblastoma									
Log (mean ± SD)	11.47±0.61	2.09±1.61	11.3±0.45	9.17±0.55	9.09±0.84	8.9±0.83	10.2±0.89	6.77±1.43	10.37±0.61
Anaplastic astrocytoma									
Log (mean ± SD)	10.46±0.70	2.78±1.54	11.10±0.44	8.77±0.55	8.19±1.14	9.03±0.71	10.12±1	4.77±2.10	9.7±0.69
Astrocytoma grade II									
Log (mean ± SD)	9.99±0.63	2.98±1.36	11.074±0.52	8.62±0.52	7.81±0.78	9.17±0.75	9.69±0.94	3.81±1.97	9.53±0.49
Normal									
Log (mean ± SD)	8.79±0.36	0.15±0.83	12.17±0.13	9.69±0.51	7.75±0.46	10.91±0.46	8.59±0.49	3.21±0.93	8.98±0.33
Glioblastoma vs. anaplastic astrocytoma									
Adjusted P-value	1.38896E-30	0.000373262	3.08282E-05	6.10399E-09	2.15289E-13	0.20064689	0.41158742	1.06584E-17	8.13945E-17
Glioblastoma vs. astrocytoma grade II									
Adjusted P-value	9.64928E-39	0.000241293	0.000199704	1.78558E-10	1.31977E-16	0.031546623	0.00035424	2.96428E-23	8.10789E-17
Glioblastoma vs. normal									
Adjusted P-value	7.41774E-16	0.013900759	0.00035894	0.068411075	0.006012107	1.76232E-07	0.000529205	7.99978E-05	7.29563E-06
Anaplastic astrocytoma vs. astrocytoma grade II									
Adjusted P-value	0.000115669	0.58144605	0.81457853	0.18047059	0.042150598	0.43026862	0.018488223	0.005033033	0.19248255
Anaplastic astrocytoma vs. normal									
Adjusted P-value	6.24305E-07	0.001064924	7.15003E-06	0.001204611	0.46713257	2.27282E-06	0.001895901	0.12621635	0.032178745
Astrocytoma grade II vs. normal									
Adjusted P-value	0.000601994	0.000684009	1.00213E-05	0.000269684	0.95525837	2.65911E-05	0.039250672	0.649572	0.1347119

Table II. Overall survival for the selected immune checkpoints in glioblastoma.

	Mean				Median				Log-rank (Mantel-Cox)	
	Estimate	SE	95% CI		Estimate	SE	95% CI		Chi-square	Significance
			Lower bound	Upper bound			Lower bound	Upper bound		
CD276										
Low	2,106.954	437.733	1,248.998	2,964.910	1,511.000	231.470	1,057.320	1,964.680		
High	1,170.322	156.700	863.189	1,477.455	1,124.000	247.168	639.551	1,608.449		
Overall	1,750.302	291.264	1,179.424	2,321.180	1,275.000	67.205	1,143.278	1,406.722	2.771	0.096
VTCN1										
Low	1,501.133	334.027	846.440	2,155.825	1,173.000	388.775	411.000	1,935.000		
High	2,332.769	419.625	1,510.304	3,155.233	1,419.000	273.388	883.160	1,954.840		
Overall	1,915.041	270.368	1,385.119	2,444.963	1,298.000	131.107	1,041.029	1,554.971	3.254	0.071
CD47										
Low	1,550.759	265.609	1,030.166	2,071.352	1,275.000	165.243	951.123	1,598.877		
High	1,563.020	348.405	880.146	2,245.894	1,101.000	292.895	526.925	1,675.075		
Overall	1,565.487	229.512	1,115.643	2,015.332	1,183.000	126.196	935.656	1,430.344	0.018	0.893
PVR										
Low	1,812.897	344.718	1,137.251	2,488.544	1,491.000	227.945	1,044.228	1,937.772		
High	1,316.999	227.311	871.470	1,762.527	1,124.000	184.382	762.612	1,485.388		
Overall	1,579.214	214.791	1,158.224	2,000.205	1,255.000	102.776	1,053.560	1,456.440	1.711	0.191
TNFRSF14										
Low	2,376.561	534.969	1,328.021	3,425.100	1,495.000	123.626	1,252.693	1,737.307		
High	1,249.227	179.475	897.456	1,600.999	1,028.000	293.848	452.057	1,603.943		
Overall	1,696.854	245.369	1,215.931	2,177.777	1,298.000	150.294	1,003.424	1,592.576	4.148	0.042
CD200										
Low	1,538.345	268.458	1,012.168	2,064.523	1,294.000	191.464	918.730	1,669.270		
High	1,960.634	491.408	997.474	2,923.794	1,419.000	184.815	1,056.762	1,781.238		
Overall	1,647.845	242.431	1,172.680	2,123.010	1,298.000	157.111	990.063	1,605.937	0.184	0.668
LGALS9										
Low	1,678.101	252.097	1,183.991	2,172.212	1,495.000	126.246	1,247.557	1,742.443		
High	1,775.014	291.699	1,203.283	2,346.744	1,403.000	234.376	943.623	1,862.377		
Overall	1,754.181	202.451	1,357.377	2,150.985	1,403.000	115.366	1,176.882	1,629.118	0.011	0.918
NECTIN2										
Low	1,914.122	383.529	1,162.406	2,665.839	1,495.000	117.504	1,264.692	1,725.308		
High	1,467.364	265.874	946.251	1,988.477	1,124.000	146.219	837.410	1,410.590		
Overall	1,693.007	232.899	1,236.525	2,149.490	1,275.000	187.661	907.184	1,642.816	1.066	0.302

Table II. Continued.

	Mean				Median				Log-rank (Mantel-Cox)	
	Estimate	SE	Lower bound	Upper bound	Estimate	SE	Lower bound	Upper bound	Chi-square	Significance
CD48										
Low	1,535.158	253.307	1,038.675	2,031.640	1,376.000	182.438	1,018.422	1,733.578		
High	1,685.861	357.415	985.327	2,386.395	1,275.000	260.223	764.962	1,785.038		
Overall	1,630.422	240.486	1,159.068	2,101.775	1,298.000	156.655	990.956	1,605.044	0.001	0.970

SE, standard error; CI, confidence interval.

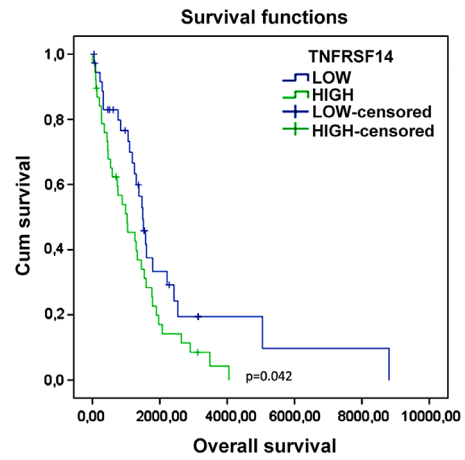


Figure 2. Effect of immune checkpoint expression on overall survival in glioblastoma. Kaplan-Meier curve for the overall survival of glioblastoma patients stratified on the expression levels of TNFRSF14.

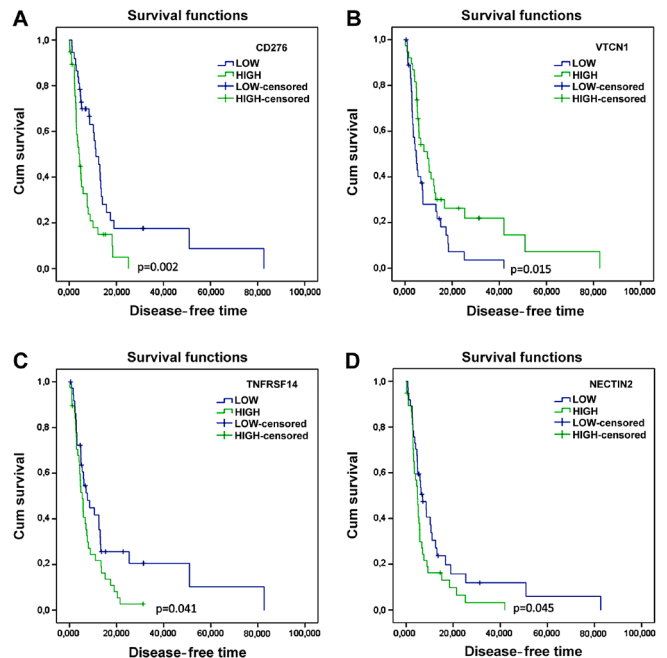


Figure 3. Effect of immune checkpoint expression on disease-free survival in glioblastoma. (A) Kaplan-Meier curve for the disease-free survival of glioblastoma patients stratified on the expression levels of CD276; (B) Kaplan-Meier curve for the disease-free survival of glioblastoma patients stratified on the expression levels of VTCN1; (C) Kaplan-Meier curve for the disease-free survival of glioblastoma patients stratified on the expression levels of TNFRSF14; (D) Kaplan-Meier curve for the disease-free survival of glioblastoma patients stratified on the expression levels of NECTIN2.

VTCN1, TNFRSF14, LGALS9, NECTIN2 and CD48 was observed in GBM as compared to normal brain samples (Fig. 1A, Table I). On the contrary, a significant downregulation of CD47 and CD200 was observed in GBM as compared to normal brain samples, while a trend of downregulation was observed for PVR (Fig. 1A, Table I). Along the same lines, with the exception of LGALS9 and CD200, a significant modulation in the expression levels of the investigated immune checkpoints was observed between the GBM and anaplastic astrocytoma groups of samples (Fig. 1A, Table I). Moreover,

Table III. Disease-free survival for the selected immune checkpoints in glioblastoma.

	Mean			Median			Log-rank (Mantel-Cox)			
	Estimate	SE	95% CI		Estimate	SE	95% CI		Chi-square	Significance
			Lower bound	Upper bound			Lower bound	Upper bound		
CD276										
Low	19.417	4.607	10.386	28.447	11.270	1.527	8.277	14.263		
High	6.726	1.132	4.507	8.945	4.300	0.760	2.810	5.790		
Overall	13.590	2.671	8.354	18.825	7.590	1.724	4.211	10.969	10.000	0.002
VTCN1										
Low	8.510	1.615	5.346	11.675	4.730	0.966	2.836	6.624		
High	19.102	4.450	10.380	27.824	9.460	2.380	4.795	14.125		
Overall	13.618	2.366	8.981	18.255	5.980	1.070	3.883	8.077	5.944	0.015
CD47										
Low	11.583	2.051	7.562	15.603	8.510	1.797	4.987	12.033		
High	11.562	2.939	5.801	17.323	5.390	0.833	3.757	7.023		
Overall	11.544	1.811	7.994	15.094	7.030	1.056	4.960	9.100	0.182	0.670
PVR										
Low	13.275	3.278	6.851	19.699	5.910	2.202	1.593	10.227		
High	6.936	1.188	4.608	9.264	4.860	0.715	3.458	6.262		
Overall	10.343	1.906	6.608	14.078	5.190	0.506	4.199	6.181	2.563	0.109
TNFRSF14										
Low	19.741	5.110	9.725	29.756	7.620	1.766	4.158	11.082		
High	7.659	1.124	5.455	9.862	5.390	0.715	3.988	6.792		
Overall	13.405	2.628	8.253	18.557	5.910	0.974	4.000	7.820	4.168	0.041
CD200										
Low	8.966	1.925	5.194	12.738	5.160	0.873	3.448	6.872		
High	17.597	4.920	7.954	27.239	8.410	1.419	5.628	11.192		
Overall	12.064	2.308	7.539	16.588	6.670	0.761	5.179	8.161	2.805	0.094
LGALS9										
Low	14.228	2.693	8.950	19.507	10.580	2.960	4.779	16.381		
High	10.808	2.001	6.887	14.729	6.340	1.336	3.722	8.958		
Overall	12.388	1.641	9.171	15.604	7.620	1.210	5.248	9.992	1.283	0.257
NECTIN2										
Low	14.843	3.950	7.101	22.584	7.030	1.789	3.524	10.536		
High	7.493	1.462	4.627	10.359	4.860	0.698	3.491	6.229		
Overall	10.843	1.991	6.942	14.745	5.190	0.480	4.249	6.131	4.010	0.045

Table III. Continued.

	Mean			Median			Log-rank (Mantel-Cox)			
	Estimate	SE	95% CI		Estimate	SE	95% CI		Chi-square	Significance
			Lower bound	Upper bound			Lower bound	Upper bound		
CD48										
Low	13.008	2.508	8.092	17.924	8.510	3.055	2.522	14.498		
High	12.505	3.101	6.426	18.584	6.410	1.560	3.352	9.468		
Overall	13.026	2.283	8.552	17.501	7.360	1.459	4.501	10.219	0.392	0.531

SE, standard error; CI, confidence interval.

CD276, TNFRSF14, LGALS9 and CD48 resulted significantly upregulated in anaplastic astrocytoma samples as compared to grade II astrocytomas (Fig. 1A, Table I). A significant direct correlation was observed for CD276, PVR, TNFRSF14, NECTIN2 and CD48 (Fig. 1B). Among the GBM samples, a significant negative correlation was instead observed between VTCN1 and PVR, NECTIN2 and CD48 (Fig. 1B).

Survival analysis. Samples were stratified in quartiles based on the expression of the genes of interest, and samples in the upper and lower quartiles were selected for comparison. As shown in Table II and Fig. 2, higher expression levels of TNFRSF14 in GBM were associated to a significantly lower overall survival. No significance was observed for any of the other immune checkpoints. Accordingly, higher TNFRSF14 levels were associated to a shorter disease-free time (Fig. 3 and Table III). Lower levels of CD276 and NECTIN2 were also significantly associated to better disease-free time (Fig. 3 and Table III). Unexpectedly, higher levels of VTCN1 were associated to a longer disease-free time (Fig. 3 and Table III).

Deconvolution analysis. Deconvolution analysis of cell infiltration in GBM was performed on samples dichotomized on the expression levels of the immune checkpoints associated to a significant modulation of survival, i.e., CD276, VTCN1, TNFRSF14 and NECTIN2. As shown in Fig. 4, higher levels of CD276, TNFRSF14 and NECTIN2 were associated with a significant lower proportion of infiltrating plasma cells. Higher VTCN1 levels were associated to higher proportions of infiltrating plasma cells, along with higher infiltration of Th1, aDCs and cDCs (Fig. 4B). Samples with high expression levels of TNFRSF14 were characterized by a significant lower infiltration of Th1 cells and cDC, and higher proportions of iDCs, aDCs, pDCs and of macrophages (both M1 and M2) (Fig. 4C). A significantly higher infiltration of iDCs, aDCs and M1 macrophages, along with reduced proportions of Th1, Th2 and CD8 T cells, were observed in GBM samples with high NECTIN2 expression levels (Fig. 4D).

Discussion

Conventional immune checkpoint inhibitors, Nivolumab/ Pembrolizumab for PD-1/PDL1 blockade or Ipilimumab for CTLA4, have proven beneficial effects on the clinical course of different cancer types, including metastatic melanoma, non-small cell lung cancer, renal cell carcinoma, and Hodgkin lymphoma (9-11). However, these treatments have often failed in gliomas (12-14). A possible explanation for this outcome seems to be due to two main glioma features: the low tumor mutational burden (TMB) and a highly immunosuppressive microenvironment. Identifying genomic markers of response to immune checkpoint may benefit cancer patients by providing predictive biomarkers for patient stratification and identifying resistance mechanisms for therapeutic targeting.

The present investigation evaluated the potential role of a series of inhibitory immune checkpoints not previously studied or only marginally characterized in GBM, i.e., CD276, VTCN1, CD47, PVR, TNFRSF14, CD200, LGALS9, NECTIN2 and CD48. To this aim, a computational analysis of RNA-seq data obtained from the TCGA (The Cancer Genome

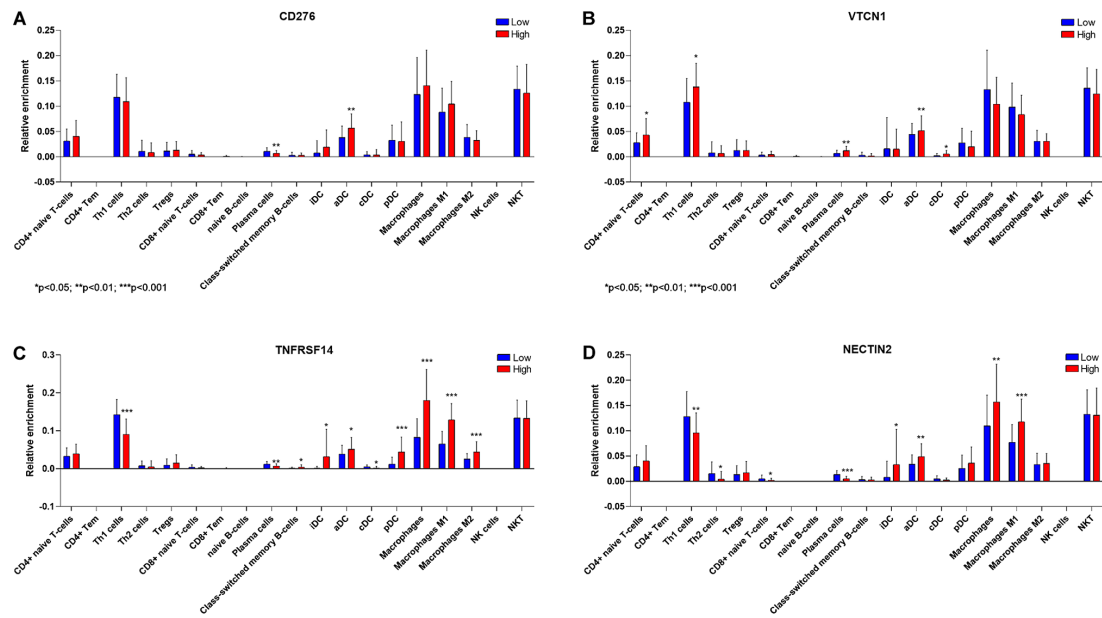


Figure 4. Deconvolution analysis of infiltrating immune cells in glioblastoma. Infiltrating immune cell populations were predicted using the web-based deconvolution analysis utility, xCell, for glioblastoma patients stratified on the expression of (A) CD276, (B) VTCN1, (C) TNFRSF14 and (D) NECTIN2. * $P < 0.05$; ** $P < 0.01$; *** $P < 0.001$.

Atlas) database was performed. Whole-genome expression data was largely used (15) to identify pathogenic pathways and therapeutic targets for several disorders, including autoimmune diseases (16-23) and cancer (24-29).

We found that VTCN1 and CD200 are highly over-expressed in GBM, anaplastic astrocytoma and astrocytoma grade II compared to normal brain. Previously, Yao *et al* (30) showed that VTCN1 has a crucial role in the creation and maintenance of the immunosuppressive microenvironment in gliomas, correlating with prognosis and malignant grades. Furthermore, lower levels of VTCN1 are associated with a higher survival in a clinical trial of DC based vaccination (31). This is in contrast with our observations, which appears to show a protective role for VTCN1 in GBM. The reasons for this counterintuitive data is currently object of further exploration.

On the contrary, CD200 expression levels resulted in significantly reduced astrocytomas in comparison to normal brain. CD200 is a type I transmembrane glycoprotein that plays an inhibitory role in the activation of microglia. For this reason, many studies have shown that its expression is enhanced in brain tumors (32), and especially in higher grade tumors (33). However, its role is still controversial, indeed in the same study Wang *et al* (33) found that CD200 down-expression can lead to a particular microglia tumor microenvironment that promotes tumor progression, in agreement with our results. Recent studies in dogs also showed that targeting CD200, enhanced the capacity of antigen-presenting cells to prime T-cells to mediate an anti-glioma response (34).

PVR and CD47 were also found down-expressed in astrocytomas when compared to normal brain, while higher levels of expression were found for LGALS9, TNFRSF14, CD48, CD276 and NECTIN2. PVR has been described as regulator of cell adhesion in a rat model of GBM (35) and a recent study in mice proved that the combination of anti-PD-1 and anti-PVR leads to a better survival (36).

CD47 is a member of the immunoglobulin superfamily that activates the signal regulatory protein- α (SIRP- α) expressed on macrophages, preventing phagocytosis. In contrast with previous studies (37,38), we found decreased levels in gliomas compared to normal brain. We consider that this down-expression can represent an attempt to maintain homeostasis. Recent studies have associated CD47 with the tumor-associated macrophages (TAMs) in the GBM microenvironment. Zhang *et al* (39) have also proven that anti-CD47 treatment leads to enhanced tumor cell phagocytosis by both M1 and M2 macrophage subtypes with a higher phagocytosis rate by M1 macrophages. A combination of anti-CD47 treatment and temozolamide has also been reported (40).

TNFRSF14 was found to be elevated in aggressive gliomas and its expression seemed to be associated with amplification of EGFR and loss of PTEN (41). TNFRSF14 plays an important role in the recruitment and activation of immune system in the tumor microenvironment. We showed that TNFRSF14 seems to have a significant impact on both the overall survival and the disease-free time. Interestingly, in metastatic melanoma, TNFRSF14 shows a similar behavior (42), further reinforcing our observations and suggesting that similar mechanisms can be shared also in glioma and that a combinatory blocking strategy can improve patients outcome.

Finally, we performed a deconvolution analysis showing that higher levels of CD276, TNFRSF14 and NECTIN2 are associated with a significant lower proportion of infiltrating plasma cells, while higher levels of VTCN1 were associated to higher proportions of infiltrating plasma cells, Th1, aDCs and cDCs. Higher levels of TNFRSF14 were associated with a major infiltration of iDCs, aDCs, pDCs and macrophages, but lower levels of Th1 cells and cDCs. Higher expression of NECTIN2, associated with shorter survival, is associated with reduced proportions of Th1, Th2 and CD8 T cells. Together these findings suggest that the main immune cell types that

help to reduce the tumor mass and improve the survival are Th1 and cDCs, and that their expression is strictly dependent on these immune checkpoints. In agreement with our hypothesis, previous studies have shown that in gliomas, there is a prevalent Th2 response and that switching from Th2 to Th1 can help to block glioma growth (43). Additionally, recent studies have proven that combinational therapy that blocks more immune checkpoints is a possibility to create a more vigorous Th1 antitumor response (44,45) and its association with better outcome (46). Future preclinical and clinical studies are necessary to ascertain whether, in addition to the prognostic value we have highlighted, the dysregulated expression of the inhibitory immune checkpoint presently studied may translate into clinical applications, as novel immunotherapeutic approaches for the treatment of gliomas and possibly other types of cancers.

Collectively, in this study, we evaluated the expression of several inhibitory immune checkpoints that can play a role in glioma progression. Among the investigated immune checkpoints, TNFRSF14 and NECTIN2 were identified as the most promising targets in GBM. In particular, TNFRSF14 expression is associated with worse overall survival and disease-free survival, correlating with a lower Th1 response and suggesting that it could become an interesting biomarker or therapeutic target.

Acknowledgements

Not applicable.

Funding

This study was supported by current research funds 2020 of IRCCS ‘Centro Neurolesi Bonino-Pulejo’, Messina, Italy.

Availability of data and materials

All the data in this study are available for download from TCGA (The Cancer Genome Atlas) databank.

Authors' contributions

Conceptualization: FN and PF; data curation: SDL, RB, KM and PF; formal analysis: MP and KM; funding acquisition: AB, PB and FN; investigation: RC; project administration: PB; supervision: FN; visualization: MSB; writing-original draft: SDL, RC, MSB, MP and RB; writing-review and editing: AB, KM, PB, FN and PF.

Ethics approval and consent to participate

Not applicable.

Patient consent for publication

Not applicable.

Competing interests

The authors declare that they have no competing interests.

References

- Louis DN, Ohgaki H, Wiestler OD, Cavenee WK, Burger PC, Jouvet A, Scheithauer BW and Kleihues P: The 2007 WHO classification of tumours of the central nervous system. *Acta Neuropathol* 114: 97-109, 2007.
- Bacher M, Schrader J, Thompson N, Kuschela K, Gemsa D, Waeber G and Schlegel J: Up-regulation of macrophage migration inhibitory factor gene and protein expression in glial tumor cells during hypoxic and hypoglycemic stress indicates a critical role for angiogenesis in glioblastoma multiforme. *Am J Pathol* 162: 11-17, 2003.
- Fritz L, Dirven L, Reijneveld JC, Koekkoek JA, Stiggelbout AM, Pasman HR and Taphoorn MJ: Advance care planning in glioblastoma patients. *Cancers (Basel)* 8: 102, 2016.
- Huang B, Zhang H, Gu L, Ye B, Jian Z, Sary C and Xiong X: Advances in immunotherapy for glioblastoma multiforme. *J Immunol Res* 2017: 3597613, 2017.
- Reardon DA, Wen PY, Wucherpennig KW and Sampson JH: Immunomodulation for glioblastoma. *Curr Opin Neurol* 30: 361-369, 2017.
- Srinivasan VM, Ferguson SD, Lee S, Weathers S-P, Kerrigan BCP and Heimberger AB: Tumor vaccines for malignant gliomas. *Neurotherapeutics* 14: 345-357, 2017.
- Sanders S and Debinski W: Challenges to successful implementation of the immune checkpoint inhibitors for treatment of glioblastoma. *Int J Mol Sci* 21: 21, 2020.
- Aran D, Hu Z and Butte AJ: xCell: Digitally portraying the tissue cellular heterogeneity landscape. *Genome Biol* 18: 220, 2017.
- Larkin J, Chiarion-Sileni V, González R, Grob J, Cowey C and Lao C: Combined nivolumab and ipilimumab or monotherapy in previously untreated melanoma. *N Engl J Med* 373: 23-34, 2015.
- Ritprajak P and Azuma M: Intrinsic and extrinsic control of expression of the immunoregulatory molecule PD-L1 in epithelial cells and squamous cell carcinoma. *Oral Oncol* 51: 221-228, 2014.
- Massari F, Santoni M, Ciccicarese C, Santini D, Alfieri S, Martignoni G, Brunelli M, Piva F, Berardi R, Montironi R, *et al*: PD-1 blockade therapy in renal cell carcinoma: Current studies and future promises. *Cancer Treat Rev* 41: 114-121, 2015.
- Tan AC, Heimberger AB and Khasraw M: Immune checkpoint inhibitors in gliomas. *Curr Oncol Rep* 19: 23, 2017.
- Desai K, Hubben A and Ahluwalia M: The role of checkpoint inhibitors in glioblastoma. *Target Oncol* 14: 375-394, 2019.
- Caccese M, Indraccolo S, Zagonel V and Lombardi G: PD-1/PD-L1 immune-checkpoint inhibitors in glioblastoma: A concise review. *Crit Rev Oncol Hematol* 135: 128-134, 2019.
- Gustafsson M, Edström M, Gawel D, Nestor CE, Wang H, Zhang H, Barrenäs F, Tojo J, Kockum I, Olsson T, *et al*: Integrated genomic and prospective clinical studies show the importance of modular pleiotropy for disease susceptibility, diagnosis and treatment. *Genome Med* 6: 17, 2014.
- Fagone P, Mazzon E, Cavalli E, Bramanti A, Petralia MC, Mangano K, Al-Abed Y, Bramati P and Nicoletti F: Contribution of the macrophage migration inhibitory factor superfamily of cytokines in the pathogenesis of preclinical and human multiple sclerosis: In silico and in vivo evidences. *J Neuroimmunol* 322: 46-56, 2018.
- Mangano K, Cavalli E, Mammana S, Basile MS, Caltabiano R, Pesce A, Puleo S, Atanasov AG, Magro G, Nicoletti F, *et al*: Involvement of the Nrf2/HO-1/CO axis and therapeutic intervention with the CO-releasing molecule CORM-A1, in a murine model of autoimmune hepatitis. *J Cell Physiol* 233: 4156-4165, 2018.
- Mammana S, Bramanti P, Mazzon E, Cavalli E, Basile MS, Fagone P, Petralia MC, McCubrey JA, Nicoletti F and Mangano K: Preclinical evaluation of the PI3K/Akt/mTOR pathway in animal models of multiple sclerosis. *Oncotarget* 9: 8263-8277, 2018.
- Fagone P, Muthumani K, Mangano K, Magro G, Meroni PL, Kim JJ, Sardesai NY, Weiner DB and Nicoletti F: VGX-1027 modulates genes involved in lipopolysaccharide-induced Toll-like receptor 4 activation and in a murine model of systemic lupus erythematosus. *Immunology* 142: 594-602, 2014.
- Nicoletti F, Mazzon E, Fagone P, Mangano K, Mammana S, Cavalli E, Basile MS, Bramanti P, Scalabrino G, Lange A, *et al*: Prevention of clinical and histological signs of MOG-induced experimental allergic encephalomyelitis by prolonged treatment with recombinant human EGF. *J Neuroimmunol* 332: 224-232, 2019.

21. Fagone P, Mazzon E, Mammanna S, Di Marco R, Spinasanta F, Basile MS, Petralia MC, Bramanti P, Nicoletti F and Mangano K: Identification of CD4⁺ T cell biomarkers for predicting the response of patients with relapsing-remitting multiple sclerosis to natalizumab treatment. *Mol Med Rep* 20: 678-684, 2019.
22. Fagone P, Mangano K, Coco M, Perciavalle V, Garotta G, Romao CC and Nicoletti F: Therapeutic potential of carbon monoxide in multiple sclerosis. *Clin Exp Immunol* 167: 179-187, 2012.
23. Patti F, Cataldi ML, Nicoletti F, Reggio E, Nicoletti A and Reggio A: Combination of cyclophosphamide and interferon- β halts progression in patients with rapidly transitional multiple sclerosis. *J Neurol Neurosurg Psychiatry* 71: 404-407, 2001.
24. Presti M, Mazzon E, Basile MS, Petralia MC, Bramanti A, Colletti G, Bramanti P, Nicoletti F and Fagone P: Overexpression of macrophage migration inhibitory factor and functionally-related genes, D-DT, CD74, CD44, CXCR2 and CXCR4, in glioblastoma. *Oncol Lett* 16: 2881-2886, 2018.
25. Fagone P, Caltabiano R, Russo A, Lupo G, Anfuso CD, Basile MS, Longo A, Nicoletti F, De Pasquale R, Libra M, *et al*: Identification of novel chemotherapeutic strategies for metastatic uveal melanoma. *Sci Rep* 7: 44564, 2017.
26. Basile MS, Mazzon E, Russo A, Mammanna S, Longo A, Bonfiglio V, Fallico M, Caltabiano R, Fagone P, Nicoletti F, *et al*: Differential modulation and prognostic values of immune-escape genes in uveal melanoma. *PLoS One* 14: e0210276, 2019.
27. Mangano K, Mazzon E, Basile MS, Di Marco R, Bramanti P, Mammanna S, Petralia MC, Fagone P and Nicoletti F: Pathogenic role for macrophage migration inhibitory factor in glioblastoma and its targeting with specific inhibitors as novel tailored therapeutic approach. *Oncotarget* 9: 17951-17970, 2018.
28. Nicoletti F, Fagone P, Meroni P, McCubrey J and Bendtzen K: mTOR as a multifunctional therapeutic target in HIV infection. *Drug Discov Today* 16: 715-721, 2011.
29. Rothweiler F, Michaelis M, Brauer P, Otte J, Weber K, Fehse B, Doerr HW, Wiese M, Kreuter J, Al-Abed Y, *et al*: Anticancer effects of the nitric oxide-modified saquinavir derivative saquinavir-NO against multidrug-resistant cancer cells. *Neoplasia* 12: 1023-1030, 2010.
30. Yao Y, Ye H, Qi Z, Mo L, Yue Q, Baral A, Hoon DSB, Vera JC, Heiss JD, Chen CC, *et al*: B7-H4(B7x)-mediated cross-talk between glioma-initiating cells and macrophages via the IL6/JAK/STAT3 pathway lead to poor prognosis in glioma patients. *Clin Cancer Res* 22: 2778-2790, 2016.
31. Yao Y, Luo F, Tang C, Chen D, Qin Z, Hua W, Xu M, Zhong P, Yu S, Chen D, *et al*: Molecular subgroups and B7-H4 expression levels predict responses to dendritic cell vaccines in glioblastoma: An exploratory randomized phase II clinical trial. *Cancer Immunol Immunother* 67: 1777-1788, 2018.
32. Moertel CL, Xia J, LaRue R, Waldron NN, Andersen BM, Prins RM, Okada H, Donson AM, Foreman NK, Hunt MA, *et al*: CD200 in CNS tumor-induced immunosuppression: The role for CD200 pathway blockade in targeted immunotherapy. *J Immunother Cancer* 2: 46, 2014.
33. Wang CY, Hsieh YT, Fang KM, Yang CS and Tzeng SF: Reduction of CD200 expression in glioma cells enhances microglia activation and tumor growth. *J Neurosci Res* 94: 1460-1471, 2016.
34. Olin MR, Ampudia-Mesias E, Pennell CA, Sarver A, Chen CC, Moertel CL, Hunt MA and Pluhar GE: Treatment combining CD200 immune checkpoint inhibitor and tumor-lysate vaccination after surgery for pet dogs with high-grade glioma. *Cancers (Basel)* 11: 137, 2019.
35. Sloan KE, Stewart JK, Treloar AF, Matthews RT and Jay DG: CD155/PVR enhances glioma cell dispersal by regulating adhesion signaling and focal adhesion dynamics. *Cancer Res* 65: 10930-10937, 2005.
36. Hung AL, Maxwell R, Theodoros D, Belcaid Z, Mathios D, Luksik AS, Kim E, Wu A, Xia Y, Garzon-Muvdi T, *et al*: TIGIT and PD-1 dual checkpoint blockade enhances antitumor immunity and survival in GBM. *OncoImmunology* 7: e1466769, 2018.
37. Li F, Lv B, Liu Y, Hua T, Han J, Sun C, Xu L, Zhang Z, Feng Z, Cai Y, *et al*: Blocking the CD47-SIRP α axis by delivery of anti-CD47 antibody induces antitumor effects in glioma and glioma stem cells. *OncoImmunology* 7: e1391973, 2018.
38. Liu X, Wu X, Wang Y, Li Y, Chen X, Yang W and Jiang L: CD47 promotes human glioblastoma invasion through activation of the PI3K/Akt pathway. *Oncol Res* 27: 415-422, 2019.
39. Zhang M, Hutter G, Kahn SA, Azad TD, Gholamin S, Xu CY, Liu J, Achrol AS, Richard C, Sommerkamp P, *et al*: Anti-CD47 treatment stimulates phagocytosis of glioblastoma by M1 and M2 polarized macrophages and promotes M1 polarized macrophages in vivo. *PLoS One* 11: e0153550, 2016.
40. von Roemeling CA, Wang Y, Qie Y, Yuan H, Zhao H, Liu X, Yang Z, Yang M, Deng W, Bruno KA, *et al*: Therapeutic modulation of phagocytosis in glioblastoma can activate both innate and adaptive antitumor immunity. *Nat Commun* 11: 1508, 2020.
41. Han MZ, Wang S, Zhao WB, Ni SL, Yang N, Kong Y, Huang B, Chen AJ, Li XG, Wang J, *et al*: Immune checkpoint molecule herpes virus entry mediator is overexpressed and associated with poor prognosis in human glioblastoma. *EBioMedicine* 43: 159-170, 2019.
42. Malissen N, Macagno N, Granjeaud S, Granier C, Moutardier V, Gaudy-Marqueste C, Habel N, Mandavit M, Guillot B, Pasero C, *et al*: HVEM has a broader expression than PD-L1 and constitutes a negative prognostic marker and potential treatment target for melanoma. *OncoImmunology* 8: e1665976, 2019.
43. Li G, Hu YS, Li XG, Zhang QL, Wang DH and Gong SF: Expression and switching of TH1/TH2 type cytokines gene in human gliomas. *Chin Med Sci J* 20: 268-272, 2005.
44. Jahan N, Talat H, Alonso A, Saha D and Curry WT: Triple combination immunotherapy with GVAX, anti-PD-1 monoclonal antibody, and agonist anti-OX40 monoclonal antibody is highly effective against murine intracranial glioma. *OncoImmunology* 8: e1577108, 2019.
45. Jahan N, Talat H and Curry WT: Agonist OX40 immunotherapy improves survival in glioma-bearing mice and is complementary with vaccination with irradiated GM-CSF-expressing tumor cells. *Neuro-oncol* 20: 44-54, 2018.
46. Taube JM, Galon J, Sholl LM, Rodig SJ, Cottrell TR, Giraldo NA, Baras AS, Patel SS, Anders RA, Rimm DL, *et al*: Implications of the tumor immune microenvironment for staging and therapeutics. *Mod Pathol* 31: 214-234, 2018.



This work is licensed under a Creative Commons Attribution-NonCommercial-NoDerivatives 4.0 International (CC BY-NC-ND 4.0) License.